Fermi surface shape and angle-dependent magnetoresistance oscillations

2001 J. Phys.: Condens. Matter 13 2271

(http://iopscience.iop.org/0953-8984/13/10/319)

INSTITUTE OF PHYSICS PUBLISHING JOURNAL OF PHYSICS: CONDENSED MATTER

J. Phys.: Condens. Matter **13** (2001) 2271–2279 www.iop.org/Journals/cm PII: S0953-8984(01)17965-8

Fermi surface shape and angle-dependent magnetoresistance oscillations

M S Nam[1], **S J Blundell, A Ardavan, J A Symington and J Singleton**

University of Oxford, Department of Physics, Clarendon Laboratory, Parks Road, Oxford OX1 3PU, UK

E-mail: s.blundell@physics.ox.ac.uk

Received 12 October 2000

Abstract

The shape of the Fermi surface of organic metals can be measured by recording angle-dependent magnetoresistance oscillations. We review this technique and develop a model for parametrizing the shape of the quasi-two-dimensional Fermi surface sections which often appear in organic metals. Using this model, we show that it is possible to extract more detail about the quasi-two-dimensional pocket shape from angle-dependent magnetoresistance oscillations than in the traditional approximation which assumes an elliptical Fermi surface shape. We also consider the implications for cyclotron resonance experiments.

1. Introduction

Organic compounds are generally insulating because they contain few charged species and exhibit poor intermolecular overlaps. Nevertheless many high-quality organic metals with well-defined Fermi surfaces, and even a large number of superconductors, have been discovered [1]. These organic conductors are surprisingly well-defined 'test-bed' materials which can be used in experiments which study superconductivity in correlated systems. A key experimental aim is to measure the dimensions and shape of the Fermi surface (FS). Measurements of magnetoresistance (MR) have been found to be extremely useful in this regard for conventional metals [2, 3]. The presence of open and closed orbits can be easily distinguished by the field dependence of the MR while the area of the FS pockets can be measured by the frequency of Shubnikov–de Haas (SdH) oscillations which is proportional to the area of an extremal orbit on the FS [3]. Such techniques are now routinely applied to organic metals [1]. The orbits which are not extremal do not contribute to this oscillatory signal but give rise to a non-oscillatory background MR. However, this background MR can depend quite dramatically on the *direction* of the applied magnetic field, and in some cases very large angle-dependent magnetoresistance oscillations (AMROs) at constant field can be found.

Experimentally, AMROs are measured by rotating a sample in a fixed magnetic field while monitoring the resistivity of the sample [4]. AMROs can be observed at much higher

[1] Present address: Department of Physics, Princeton University, Princeton, NJ 08544, USA.

0953-8984/01/102271+09$30.00

temperatures and in much lower applied fields than SdH oscillations. This is because SdH oscillations arise from the movement of Landau levels through the Fermi energy (E_F) and therefore require that the temperature is low enough for the FS to be sharply defined; this restriction does not apply so stringently to AMROs since they do not originate from the motion of energy levels through the FS. The information obtained from AMROs can therefore be complementary to SdH oscillations since the effect is due to all electrons on the FS, not just those performing extremal orbits [5]. In the case for which the quality of a sample of an organic metal is too poor to allow the measurement of SdH oscillations, AMROs can nevertheless be measured and thus allow information about FS shapes to be obtained [6]. In this paper we demonstrate how measurements of AMROs can lead to a determination of FS shape (section 2) and present a method of parametrizing the shape of FS pockets (section 3) which can be applied to an organic metal. We also consider implications for cyclotron resonance experiments (section 4).

2. Open and closed orbits and AMROs

In order to calculate galvanomagnetic effects in a metal, a necessary preliminary is to understand which electron orbits are possible across the FS for a given orientation of the magnetic field. Then, the conductivity σ_{ij} can be calculated using the Boltzmann transport equation:

$$\sigma_{ij} = \frac{e^2}{4\pi^3} \int \mathrm{d}^3\boldsymbol{k} \left[-\frac{\partial f_0(\boldsymbol{k})}{\partial E(\boldsymbol{k})} \right] v_i(\boldsymbol{k}, 0) \int_{-\infty}^{0} v_j(\boldsymbol{k}, t) \mathrm{e}^{t/\tau} \, \mathrm{d}t. \tag{1}$$

It has been found that weakly incoherent transport theories also predict very similar AMROs, so a three-dimensional FS is not necessary to explain this effect [7, 8]. Nevertheless the use of the Boltzmann transport equation greatly simplifies the discussion and is more straightforward to calculate. Equation (1) is an integral (over all states at the FS) of the velocity–velocity correlation function for each FS orbit. This can change dramatically as the direction of the magnetic field is changed, because this alters the paths of all the FS orbits. It can be particularly sensitive to whether the orbits are open or closed, so these two cases may be distinguished by differing MR behaviour. They will be considered in turn below.

2.1. Open orbits

Open orbits are usually obtained by electron motion along corrugated sheets in the FS. In this case the AMROs are connected with the fact that for any Fourier component of corrugation, the velocity is more effectively averaged when electrons are not travelling along the axis of the corrugation than when they are; sharp resistance minima are obtained when the orbits run along a Fourier component of the corrugation [9, 10]. Thus the geometry of the Fermi sheet, parametrized by the Fourier components t_{mn} of the corrugation, entirely controls the AMROs. In fact it seems that quasi-1D Fermi sheets in organic materials are almost always insufficiently corrugated to give strong AMRO features. This is because the Fourier components are related to transfer integrals and these fall off very quickly with distance as one goes beyond the nearest-neighbour level [10–12]. Nevertheless such AMROs can be observed if the FS is highly corrugated. This can occur if, for example, it is a reconstructed FS obtained by nesting (i.e. cutting and pasting together) quasi-two-dimensional pieces of FS. This is believed to be the case in α-(BEDT-TTF)$_2$KHg(SCN)$_4$ [13, 14].

If an organic material has only a weakly warped Fermi sheet without high-order transfer integrals (as in the case of the TMTSF salts), AMROs are only expected to be observed if

the magnetic field is rotated close to the direction perpendicular to the sheets (i.e. close to the highly conducting direction). In this case oscillations may be observed which are associated with open orbits which weave between islands of closed orbits around the local maxima and minima (around the local hillocks and valleys on the sheets) (reference [15]; see also [10, 16]). These oscillations have been experimentally observed in $(TMTSF)_2ClO_4$ by Danner, Kang and Chaikin by rotating the magnetic field close to the a-axis [15]. An additional effect (known as the third angular effect) is expected when the field is rotated in the most conducting plane and also originates from the vanishing of closed orbits on the FS sheets [17, 18].

2.2. Closed orbits

Consider now the AMROs due to a warped cylindrical FS pocket lying along the k_z-direction. This situation applies to many salts based upon the organic molecule BEDT-TTF [1]. The electron dispersion can in this case be written as

$$E(\boldsymbol{k}) = \mathcal{E}(\boldsymbol{k}_\parallel) - 2t\cos(k_z d) \tag{2}$$

where $\boldsymbol{k}_\parallel = (k_x, k_y)$ and k_z are respectively the components of the wave vector parallel and perpendicular to the conducting planes. If the magnetic field is perpendicular to the planes, both neck and belly orbits will occur around the FS. It was realized by Yamaji that at certain inclination angles of the magnetic field (for the case $\mathcal{E}(\boldsymbol{k}_\parallel) = (\hbar^2/2m)(k_x^2 + k_y^2)$ this is given by $k_F d\tan\theta = \pi(n - 1/4)$, where n is an integer) all orbits will have identical area S which he argued could produce AMRO peaks because the SdH-oscillation amplitude would be largest at these angles [19]. This explained the AMROs which had been previously observed in β-ET_2IBr_2 [20, 21] and θ-ET_2I_3 [22]. However, since the effect is seen at higher temperatures than SdH oscillations, the concept of constant cross-sectional *area* maximizing the SdH-oscillation amplitude is not primarily relevant. Rather one can use the Boltzmann equation (equation (1)) to calculate the conductivity for all orbits around the FS for arbitrary field orientation [4, 23]. The equivalence of the two approaches was shown in [4]: the average velocity perpendicular to the 2D layers is proportional to $\partial S/\partial K_z$ (where K_z labels the k_z-position of the centre of the orbit) and thus vanishes when S is not a function of K_z. In this way one can show that Yamaji's result is nevertheless correct and the AMRO peaks are connected with the vanishing of the electronic group velocity perpendicular to the 2D layers. The angles θ_n at which the maxima occur are given by $k_\parallel^{max} d\tan(\theta_n) = \pi(n \pm 1/4) + A(\phi)$, where the signs $-$ and $+$ correspond to positive and negative θ_n respectively, d is the effective interplane spacing, $k_\parallel^{max}$ is the maximum Fermi wave-vector projection on the plane of rotation of the field, and $n = \pm 1, \pm 2, \ldots$ [4]. Here positive n correspond to $\theta_n > 0$ and negative n to $\theta_n < 0$ [4]. The gradient of a plot of $\tan\theta_n$ against n may thus be used to find one of the dimensions of the FS and, if the process is repeated for several planes of rotation of the field, the complete FS may be mapped out. $A(\phi)$ is determined by the inclination of the plane of warping; hence this may also be found [4].

This approach has been used to study many organic metals, including the organic superconductor κ-$(BEDT\text{-}TTF)_2Cu(SCN)_2$ which has both quasi-one-dimensional and quasi-two-dimensional sections of FS [24]. It has also been calculated for the superconductor $Tl_2Ba_2CuO_6$ [25]. In these experiments, the shapes of quasi-2D FS pockets can be deduced by AMRO measurements. For each azimuthal angle, ϕ, one performs a caliper measurement of the FS. (See figure 1.) The conventional way to do this is to assume an elliptical FS pocket given by

$$\left|\frac{k_x}{k_a}\right|^2 + \left|\frac{k_y}{k_b}\right|^2 = 1 \tag{3}$$

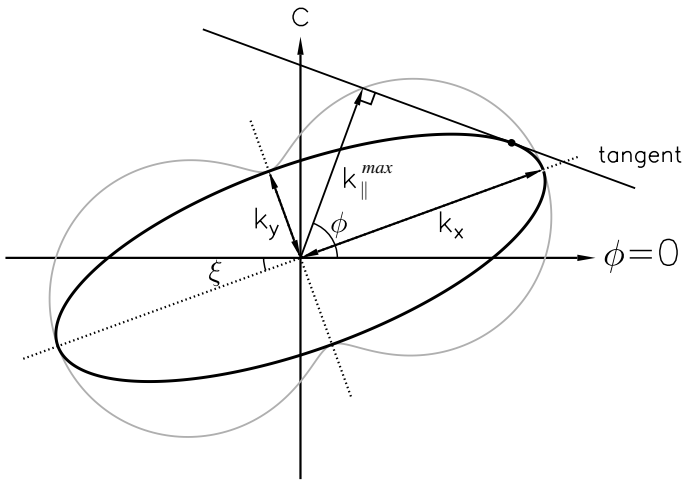

Figure 1. Caliper measurement of the Fermi surface.

where k_a and k_b are the lengths of the principal axes of the ellipse (which is assumed to be in the a–b plane). Hence the caliper measurement yields [26]

$$k_\parallel^{max} = [k_a^2 \cos^2\phi + k_b^2 \sin^2\phi]^{1/2}. \tag{4}$$

These techniques have mainly been applied to extract the parameters of pockets that are assumed to be elliptical. However, band-structure calculations often predict non-elliptical pocket shapes; it is instructive to consider the effect of non-ellipticity on the AMROs generated by a more general Q2D Fermi surface, and this will be presented in the following section.

3. Quasielliptical pockets

A generalization of the elliptical FS pocket shape which interpolates between an elliptical and rectangular shape is motivated by a geometrical construct known as a 'superellipse' proposed by Piet Hein [27] which involves an additional parameter n. We therefore consider the case of a pocket whose shape is given by the equation

$$\left|\frac{k_x}{k_a}\right|^n + \left|\frac{k_y}{k_b}\right|^n = 1. \tag{5}$$

When $n = 2$ the pocket is elliptical, but for other values of the exponent n it may take on other shapes. If $n \leqslant 1$ the pocket is concave. The shapes given by alternative choices of n are shown in figure 2. The area of the pocket is given by

$$S = 4\int_0^{k_a} k_y \, \mathrm{d}k_x \tag{6}$$

$$= 4k_b \int_0^{k_a} \left[1 - \left(\frac{k_x}{k_a}\right)^{1/n}\right] \mathrm{d}k_x \tag{7}$$

$$= \frac{4k_a k_b}{n} \frac{\Gamma(1/n)\Gamma(1/n+1)}{\Gamma(2/n+1)} \tag{8}$$

which reduces to $\pi k_a k_b$ in the case of $n = 2$. When $n = 1$ the FS pocket is a diamond shape and the area is then $2k_a k_b$. The area as a function of n is plotted in figure 3.

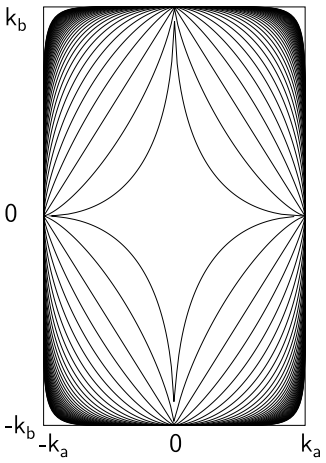

Figure 2. Pocket shapes given by $|k_x/k_a|^n + |k_y/k_b|^n = 1$ for different values of n. When $n < 1$ the superellipses are concave; when $n = 1$ the superellipse is diamond shaped. When $n = 2$ an ellipse is obtained. As $n \to \infty$ the superellipse develops rounded corners and gradually fills out into a rectangle.

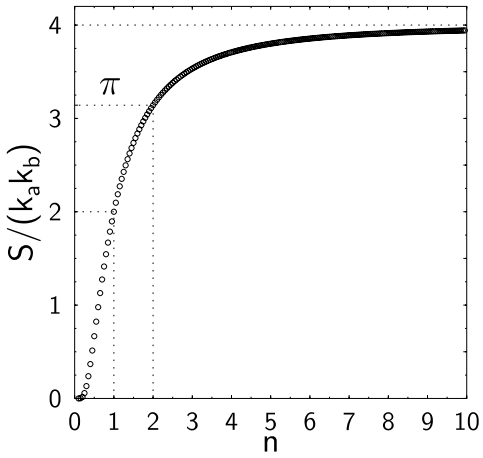

Figure 3. The area of the pocket as a function of n.

A caliper measurement of the FS pocket can be used to measure the area in the case when $n \geqslant 1$. If $n < 1$ then the caliper measurement will provide a result as if $n = 1$ because the FS is concave. We find that the caliper measurement provides a measure of the FS diameter given by

$$k_{\parallel}^{max} = \frac{\sin\phi + \cos\phi[(k_a/k_b)^n \cot\phi]^{1/(n-1)}}{([k_a \cot\phi/k_b^n]^{n/(n-1)} + k_b^{-n})^{1/n}} \tag{9}$$

which reduces to equation (4) for the case in which $n = 2$.

A further degree of freedom in the shape of the FS pocket can be obtained by introducing a shearing parameter ξ. In this case, the FS pocket can be of the form

$$\left|\frac{k_x}{k_a}\right|^n + \left|\frac{k_y + \xi k_x}{k_b}\right|^n = 1. \tag{10}$$

This results in a more complicated expression for the angular dependence of $k_{\|}$. This can be fitted to real data with k_a, k_b, n and ξ as fitting parameters.

We have applied the model to the analysis of the AMROs in the organic superconductor β''-(BEDT-TTF)$_2$SF$_5$CH$_2$CF$_2$SO$_3$. This is one of only a few purely organic superconductors ($T_c \sim 5.2$ K) [28,29] with a large anion which contains no solvent molecules. In the β''-phase structure, the BEDT-TTF molecules are nearly parallel to each other and are separated by the anion layer. The electronic properties of β''-(BEDT-TTF)$_2$SF$_5$CH$_2$CF$_2$SO$_3$ are not very well known. According to band-structure calculations [29], its Fermi surface (FS) contains a pair of quasi-one-dimensional Fermi sheets and a Fermi pocket corresponding to a quantum-oscillation frequency of 600 T, or about 25% of the first Brillouin zone. However, SdH oscillations [30–32], AMROs [30, 33] and cyclotron resonance (CR) [33] suggest a smaller pocket corresponding to a frequency of around 200 T.

Figure 4(a) shows AMRO data obtained on this salt at 10 T and a temperature of 1.5 K. The data show a striking dependence on the orientation of the magnetic field. The $\tan\theta$ periodicity of each trace is used to obtain a 'caliper' measurement of $k_{\|}^{max}$, and figure 4(b) shows the FS pocket geometry resulting from fits to equation (9) for the case when n is a free parameter (solid line; the fit gives $n = 1.1$). The fitted FS has $k_a = 2.26 \times 10^9$ m^{-1} and $k_b = 0.39 \times 10^9$ m^{-1}, giving an area corresponding to a quantum-oscillation frequency of 196 T, in excellent agreement with the Shubnikov–de Haas oscillation frequency of 198 ± 1 T obtained in the same experimental run. This is rather superior to the fit obtained when $n = 2$ [30].

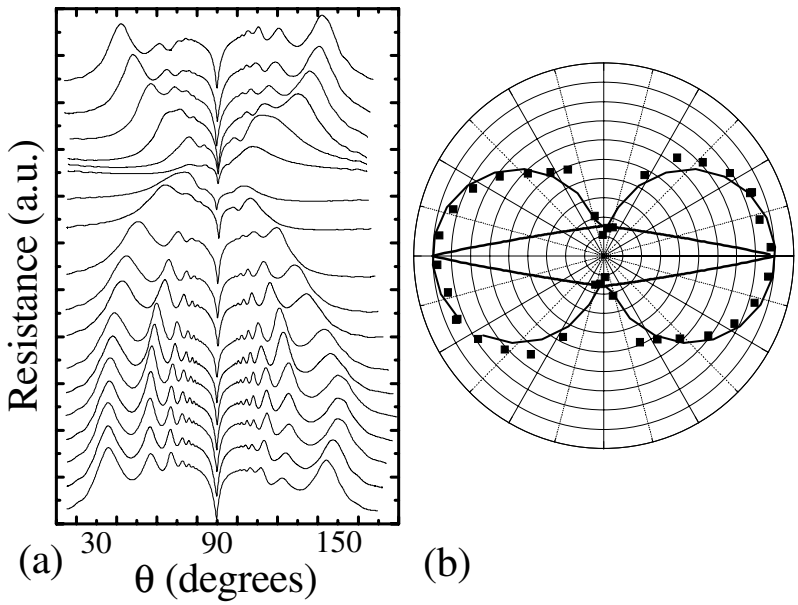

Figure 4. (a) AMRO data for β''-(BEDT-TTF)$_2$SF$_5$CH$_2$CF$_2$SO$_3$ at 10 T and 1.5 K for ϕ-angles $7 \pm 1^\circ$ (top trace), $17 \pm 1^\circ$, $27 \pm 1^\circ$, ..., $177 \pm 1^\circ$ (bottom trace); adjacent traces are spaced by $10 \pm 1^\circ$. Here $\phi = 0$ corresponds to rotation in the $\boldsymbol{a}^*\boldsymbol{c}^*$-plane of the crystal. The resistance was measured using a low-frequency ac current of 5 μA applied in the interplane direction; in this geometry, the measured resistance is proportional to the interplane resistivity component ρ_{zz} [1]. (b) The ϕ-dependence of $k_{\|}^{max}$ deduced from the $\tan\theta$ periodicity of the AMRO in (a) (points); the 'figure of eight' solid curve is a fit. The resulting fitted Fermi surface pocket (elongated diamond shape; $n = 1.1$) is shown within. The long axis of the pocket makes an angle of $144 \pm 3^\circ$ with the $\boldsymbol{a}^*$-axis.

4. Cyclotron resonance

So far we have only considered the dc conductivity due to velocity–velocity correlations along orbits around the FS. However, the real-space velocity associated with a quasi-two-dimensional orbit is a periodic function because the orbit is periodic. Hence each component of the velocity can be expressed as a Fourier series [35]:

$$v_x(t) = \sum_{m=1}^{\infty} v_m \cos(m\omega_c t + \phi_m). \tag{11}$$

The time evolution of the real-space velocity is reflected in the bulk high-frequency conductivity through Chambers' formula [35–37]. Each harmonic in the real-space velocity generates a cyclotron resonance (CR) in the conductivity; each non-zero v_m in equation (11) causes a CR in $\sigma_{xx}(\omega)$ at a frequency of $\omega = m\omega_c$. This frequency-dependent transport can be measured using millimetre waves in resonant cavities.

In figure 5 we illustrate this by showing the time dependence of the real-space velocity for quasiparticles orbiting the FS in equation (5) for $k_a = k_b = 1$. Since equation (5) defines only the FS shape and provides no information about the band dispersion local to the FS, we work in a linearized approximation, such that the magnitude of the real-space velocity remains

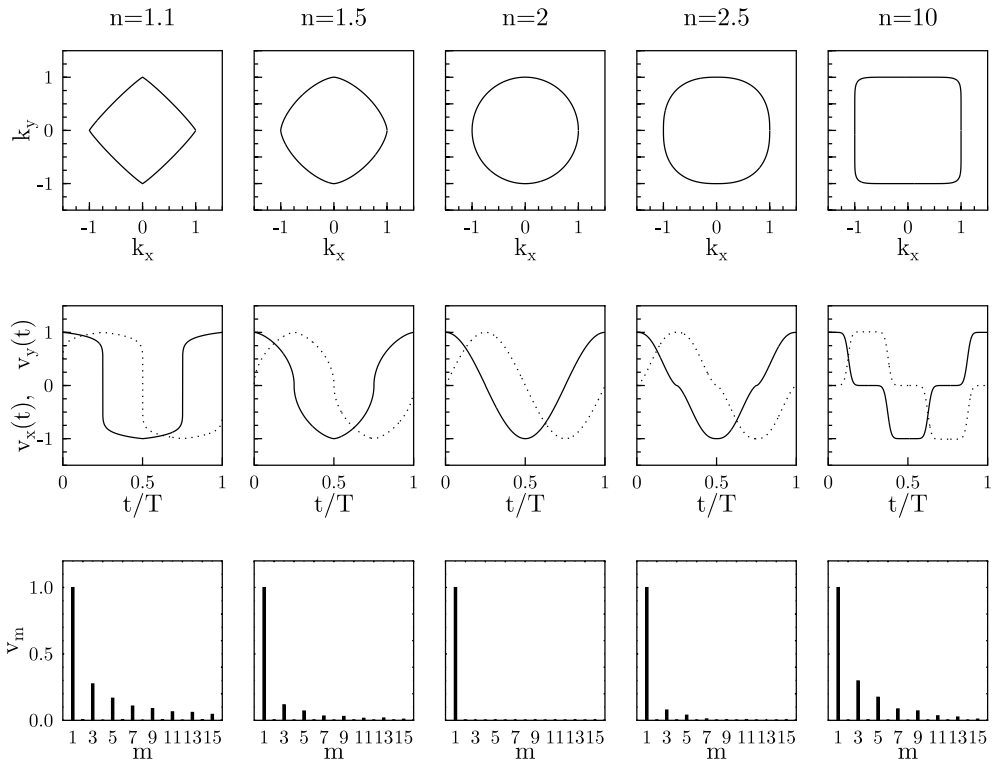

Figure 5. Orbits around the Fermi surface for $k_a = k_b$ and for a range of n. The top row shows the orbits in k-space; the middle row shows the time dependence of the velocity components along the x- and y-directions as a function of time, measured in units of the cyclotron period $T = 2\pi/\omega_c$. The lower panel shows the amplitude of the Fourier components of the real-space velocities of electrons orbiting the Fermi pockets which controls the amplitude of cyclotron resonances at $\omega = m\omega_c$. Only odd harmonics are produced.

constant over the FS. When $n = 2$ the orbit is circular and the real-space velocity contains only the fundamental frequency. When n departs significantly from 2, odd higher harmonics of the cyclotron frequency are produced in the real-space velocity which could couple to the millimetre waves; even harmonics are suppressed by the symmetry of the orbit. A related effect known as the Fermi surface traversal resonance (FTR) is produced for open electronic orbits over quasi-one-dimensional sections of FS [35,38–40]. This is not a CR since no closed orbit is involved. FTRs have been observed experimentally [41]. The effect described in this paper has not yet been definitively observed (though there is a tantalizing indication of this effect in Sr_2RuO_4 [42]), but experiments are currently under way in order to search for high CR harmonics in FSs which depart significantly from pure circular or elliptical shapes.

5. Conclusions

In conclusion, we have proposed a new parametrization of the FS shape which is simple to apply to real experimental data and provides additional information about the FS shape from AMRO experiments. The FS shape is crucial in determining ground-state properties depending on electron–electron interactions. This approach extends the applicability of AMRO as a tool for fermiological studies.

Acknowledgments

We would like to thank the EPSRC for financial support. We are indebted to Bill Hayes for numerous discussions about the physics of organic metals.

References

[1] Singleton J 2000 *Rep. Prog. Phys.* **63** 1111
[2] Pippard A B 1989 *Magnetoresistance in Metals* (Cambridge: Cambridge University Press)
[3] Shoenberg D 1984 *Magnetic Oscillations in Metals* (Cambridge: Cambridge University Press)
[4] Kartsovnik M V, Laukhin V N, Pesotskii S I, Schegolev I F and Yakovenko V M 1992 *J. Physique* I **2** 89
[5] Blundell S J and Singleton J 1996 *J. Physique* I **6** 1837
[6] Blundell S J, House A A, Singleton J, Kurmoo M, Pratt F L, Pattenden P A, Hayes W, Graham A W, Day P and Perenboom J A A J 1997 *Synth. Met.* **85** 1569
[7] McKenzie R H and Moses P 1999 *Phys. Rev.* B **60** R11 241
[8] Moses P and McKenzie R H 1999 *Phys. Rev.* B **60** 7998
[9] Osada T, Yagi R, Kawasumi A, Kagoshima S, Miura N, Oshima M and Saito G 1990 *Phys. Rev.* B **41** 5428
[10] Blundell S J and Singleton J 1996 *Phys. Rev.* B **53** 5609
[11] Osada T, Kawasumi A, Kagoshima S, Miura N and Saito G 1991 *Phys. Rev. Lett.* **66** 1525
[12] Osada T 1997 *Synth. Met.* **86** 2143
[13] Caulfield J, Singleton J, Hendriks P T J, Perenboom J A A J, Pratt F L, Doporto M, Hayes W, Kurmoo M and Day P 1994 *J. Phys.: Condens. Matter* **6** 155
[14] House A A, Blundell S J, Honold M M, Singleton J, Perenboom J A A J, Hayes W, Kurmoo M and Day P 1996 *J. Phys.: Condens. Matter* **8** 8829
[15] Danner G M, Kang W and Chaikin P M 1994 *Phys. Rev. Lett.* **72** 3714
[16] Danner G M, McKernan S, Shi X D, Kang W, Hannahs S T and Chaikin P M 1995 *Synth. Met.* **70** 731
[17] Osada T, Kagoshima S and Miura N 1996 *Phys. Rev. Lett.* **77** 5261
[18] Hanasaki N, Kagoshima S, Hasegawa T, Osada T and Miura N 1998 *Phys. Rev.* B **57** 1336
[19] Yamaji K 1989 *J. Phys. Soc. Japan* **58** 1520
[20] Kartsovnik M V, Kononovich P A, Laukhin V N and Schegolev I F 1988 *JETP Lett.* **48** 541
[21] Schegolev I F, Kononovich P A, Laukhin V N and Kartsovnik M V 1989 *Phys. Scr.* T **29** 46
[22] Kajita K, Nishio Y, Takahashi T, Sasaki W, Kato R, Kobayashi H, Kobayashi A and Iye Y 1989 *Solid State Commun.* **70** 1189
[23] Peschansky V G, Lopez J A R and Yao T G 1991 *J. Physique* I **1** 1469

[24] Nam M S, Honold M M, Proust C, Harrison N, Mielke C H, Blundell S J, Singleton J, Hayes W, Kurmoo M and Day P 1999 *Synth. Met.* **103** 1905
[25] Dragulescu A, Yakovenko V M and Singh D J 1999 *Phys. Rev.* B **60** 6312
[26] House A A, Harrison N, Blundell S J, Deckers I, Singleton J, Herlach F, Hayes W, Perenboom J A A J, Kurmoo M and Day P 1996 *Phys. Rev.* B **53** 9127
[27] Gardner M 1965 *Sci. Am.* **213** (3) 222
[28] Schlueter J A, Geiser U, Williams J M, Dudek J D, Kelly M E, Flynn J P, Wilson R R, Zakowicz H I, Sche P P, Naumann D, Roy T, Nixon P G, Winter R W and Gard G L 1997 *Synth. Met.* **85** 1453
[29] Geiser U, Schlueter J A, Wang H H, Kini A M, Williams J M, Sche P P, Zakowicz H I, Van Zile M L, Dudek J D, Nixon P G, Winter R W, Gard G L, Ren J and Whangbo M H 1996 *J. Am. Chem. Soc.* **118** 9996
[30] Beckmann D, Wanka S, Wosnitza J, Schlueter J A, Williams J M, Nixon P G, Winter R W, Gard G L, Ren J and Whangbo M H 1998 *Eur. Phys. J.* B **1** 295
[31] Zuo F, Su X, Zhang P, Brooks J S, Wosnitza J, Schlueter J A, Williams J M, Nixon P G, Winter R W and Gard G L 1999 *Phys. Rev.* B **60** 6296
[32] Nam M S, Ardavan A, Symington J A, Singleton J, Harrison N, Mielke C H, Schleuter J A and Williams J M 2001 *Phys. Rev. Lett.* submitted
[33] Schrama J M, Singleton J, Edwards R S, Ardavan A, Rzepniewski E, Goy P, Harris R, Schleuter J A, Kurmoo M and Day P 2001 *J. Phys.: Condens. Matter* **13** 2235
[34] Wosnitza J, Wanka S, Hagel J, Balthes E, Harrison N, Schlueter J A, Kini A M, Geiser U, Mohtasham J, Winter R W and Gard G L 2000 *Phys. Rev.* B **61** 7383
[35] Blundell S J, Ardavan A and Singleton J 1997 *Phys. Rev.* B **55** R6129
[36] Olszewski S, Rolinski T and Kwiatkowski T 1999 *Phys. Rev.* B **59** 3740
[37] Hill S 1997 *Phys. Rev.* B **55** 4931
[38] McKenzie R H and Moses P 1998 *Phys. Rev. Lett.* **81** 4492
[39] Ardavan A, Blundell S J and Singleton J 1999 *Phys. Rev.* B **60** 15 500
[40] Ardavan A, Singleton J and Blundell S J 2001 *Synth. Met.* at press
[41] Ardavan A, Schrama J M, Blundell S J, Singleton J, Hayes W, Kurmoo M, Day P and Goy P 1998 *Phys. Rev. Lett.* **81** 713
[42] Ardavan A, Edwards R S, Rzepniewski E, Singleton J and Blundell S J 2001 *Physica* B at press